ELSEVIER

Polymer 42 (2001) 8565–8570

polymer

www.elsevier.com/locate/polymer

Chain dynamics and stability of the poly (3-methacryloxypropyltrimethoxysilane-*co*-vinylimidazole)

T.C. Chang[a,*], T.F. Yeh[a], C.W. Yang[a], Y.S. Hong[a], T.R. Wu[b]

[a]*Department of Applied Chemistry, Chung Cheng Institute of Technology, National Defense University, Tahsi, Taoyuan 335, Taiwan, ROC*
[b]*Chemical Systems Research Division, Chung Shan Institute of Science and Technology, Lungtan, Taoyuan 325, Taiwan, ROC*

Received 19 February 2001; received in revised form 10 May 2001; accepted 21 May 2001

Abstract

The chain dynamics and the apparent activation energy of dehydration and decomposition of the ester bond for poly(3-methacryloxypropyl-trimethoxysilane-*co*-vinylimidazole) copolymer (PMPS–PVI), were examined by high-resolution solid-state ^{29}Si and ^{13}C nuclear magnetic resonance spectroscopy and thermogravimetric analysis (TGA). The $^{29}Si-^{1}H$ cross-polarization process revealed that the 3-methacryloxypropyltrimethoxysilane (MPS) components species had similar CP efficiency. The spin–lattice relaxation time in rotating frame ($T_{1\rho}^{H}$) of the copolymers indicated that the molecular motion of the imidazole ring was independent of the MPS content. The apparent activation energy of dehydration under nitrogen was dependent on the MPS content, while that of decomposition ester bond was independent of the MPS content.

Keywords: Vinylimidazoe; Methacryloxysilane; Copolymer

1. Introduction

The effectiveness of heterocyclic molecules as corrosion inhibitor is based on their chelating action and the formation of an insoluble physical diffusion barrier on metal surface, preventing metal reaction. Nitrogen-containing heterocyclic molecules due to the strong π-interaction between the aromatic rings readily form such a barrier. The most used among them are benzotriazole [1], benzimidazole [2] and tetrazole [3]. The small nitrogen-containing heterocyclic molecules lost their effectiveness as high temperature due to evaporation. Moreover, polyvinylimidazole (PVI) is interesting to working with because it is relatively simple to synthesis [4–7]. A weakness of PVI, and other imidazoles similar to it, is that they are sensitive to humidity. Therefore, the trimethoxysilane-modified vinylimidazole copolymer with moisture resistance is further synthesized [8–14]. The chain dynamics, dehydration and degradation of this copolymer provide important additional information for its use and applications as an anticorrosion coating, curing agent, ion-exchange resin, humidity sensor and matrix for magnetic nanocomposites. However, only a few paper concerning the stability of the trimethoxysilane-modified vinylimidazole copolymer [11,13] and the chain dynamics of the polymer complex of PVI and poly(methacrylic acid) [15].

Several factors, such as the change of molecular mass, addition of a suitable polymer modifier, preparation of polymer complex, spinning in different conditions, and stretching [16,17] can influence the chain dynamics of the polymer. Nuclear magnetic resonance (NMR) relaxation time measurements are sensitive to short range interactions, and are possible to estimate the scale of miscibility of an inorganic–organic hybrid [18]. The Si–H polarization transfer relaxation time constant (T_{SiH}) can be calculated from a double exponential fit of the NMR line intensity versus contact time. On the other hand, the technique of the rotating frame spin–lattice relaxation times ($T_{1\rho}^{H}$), owing to the low frequency and the restriction of spin-diffusion over the much shorter $T_{1\rho}$ times, is more sensitive to the structural changes and molecular motions than those of the laboratory frame spin–lattice relaxation times (T_1) [16]. To understand the effect of 3-methacryloxypropyl-trimethoxysilane (MPS) monomer content on the chain dynamics of the poly(3-methacryloxypropyl-trimethoxy-silane-*co*-vinylimidazole) copolymers (PMPS–PVI), we have measured relaxation times of T_{SiH} and $T_{1\rho}^{H}$, respectively. Additionally, the effect of MPS content on the dehydration and degradation of the copolymers in nitrogen has been also investigated by thermogravimetric analysis (TGA). The values of apparent activation energy E_a for

* Corresponding author.
E-mail address: techuan@ccit.edu.tw (T.C. Chang).

0032-3861/01/$ - see front matter
PII: S0032-3861(01)00435-9

dehydration and degradation of MPS segments under nitrogen have been estimated employing the method of van Krevelen [19], Coats–Redfern [20], and MacCallum–Tanner [21], respectively.

2. Experimental

2.1. Materials

The monomer vinylimidazole (VI; TCI) was purified by distillation before use. 3-Methacryloxypropyltrimethoxysilane (MPS; TCI) was used without purification. Azoisobutyronitrile (AIBN; BDH) was recrystallized from ethanol just before use. Tetrahydrofuran (THF; Aldrich) was fractionally distilled in the presence of calcium hydride under nitrogen atmosphere.

2.2. Copolymerization

The copolymerization scheme of MPS and vinylimidazole (VI) is presented in Scheme 1. For a typical example, a mixture of VI (95 mmol; 8.9414 g) and MPS (5 mmol; 1.2418 g), AIBN (0.1 mmol) and THF (70 ml) was poured into a 250 ml round bottom flask under nitrogen, and the solution was stirred at 60°C (8 h) to initiate the copolymerization of the monomers. A large volume of n-hexane precipitated the resulting homogeneous mixture. The precipitated copolymer was collected by filtration, washed with THF, and dried. After drying at room temperature for 24 h under atmospheric pressure, the copolymer was dried in vacuum oven for 24 h. Copolymer PMPS(5)–PVI was then obtained, where 5 donates that 5 mol% of MPS copolymerized with 95 mol% of VI based on mole of monomer. Copolymers PMPS(10)–PVI, PMPS(15)–PVI, PMPS(20)–PVI, PMPS(25)–PVI and PMPS(30)–PVI were also prepared for comparison comprising 10, 15, 20, 25 and 30 mol% MPS, respectively.

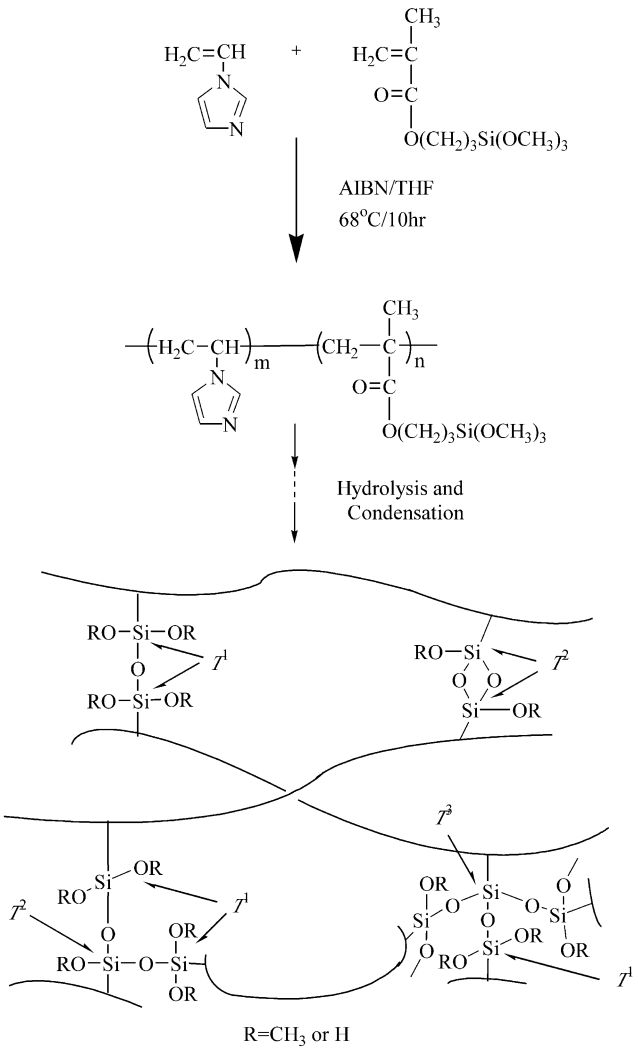

PMPS-PVI Copolymer

Scheme 1.

2.3. Characterization

PMPS–PVI copolymer was confirmed by infrared (IR) spectrum (Bomem DA 3.002) of sample prepared as KBr pellets technique. The ^{13}C and ^{29}Si NMR spectra of the solid-state PMPS–PVI copolymers were determined (Bruker MSL-400) by using the cross-polarization combined with magic angle spinning (CP/MAS) technique. T^i denotes species that have one organic side group where i refers to the number of –O–Si groups bounded to the silicon atom of interest. The relative proportions of the T^i-species were calculated on the basis of the experimental spectra. CP contact time studies can produce Si–H polarization transfer constant (T_{SiH}). The ^1H–^{29}Si spin contact time with the Hartmann–Hahn condition fulfilled in the rotating frame was typically about 5 ms, but optimized in the range between 0.1 and 20 ms. Proton spin–lattice relaxation time in the rotating frame ($T_{1\rho}^H$) were measured by using a ^1H spin-lock τ-pulse sequence followed by the cross-polarization. The ^1H 90° pulse width was 4.5 μs, and the CP contact time was 2 ms. The length of delay time τ was range from 0.1 to 10 ms for $T_{1\rho}^H$. Differential scanning calorimetry (DSC) was conducted in a Perkin–Elmer 7 unit. The sample weight was 8 mg and the scanning rate was 10°C/min under nitrogen. The characteristics and kinetics of degradation of PMPS–PVI copolymers were measured by a Perkin–Elmer TGA-2 at heating rate of 10°C/min under nitrogen and air. The sample weight was about 10 mg, and the gas flow rate was kept at 100 ml/min.

3. Results and discussions

Evidence for the formation of copolymers is provided by FTIR, DSC, solid-state ^{13}C and ^{29}Si NMR. All copolymers present the characteristic VI peaks (3112, 1496, 1227, and

655 cm^{-1}) and MPS peaks (1709 and 1282 cm^{-1}) [22]. The absorption in the range 3700–3200 cm^{-1} and 950 cm^{-1} in copolymers is assigned to the silanol groups (Si–OH) that is formed during the hydrolysis of methoxyl groups in MPS. The peaks at 3112 and 1496 cm^{-1}, respectively originate from the C=C–H/N=C–H and C=C/C=N stretching. Moreover, the peaks at 1227 and 655 cm^{-1} are due to the ring vibration and torsion stretching, respectively. However, the peaks at 1709 and 1282 cm^{-1} are associated with the ester functionality of MPS.

3.1. Si–H polarization transfer constant T_{SiH}

^{29}Si NMR spectra of the PMPS–PVI copolymers show three peaks about at −49, −57 and −66 ppm corresponding to T^1, T^2 and T^3 structure, respectively. The relative proportion of T^2 (~52%) and T^3 (~14%) in copolymers, determined by a quantitative analysis of the resonance signals, is independent of the MPS content (Table 1). The peaks at T^2 and T^3 reveal that the methoxyl groups undergo hydrolysis and condensation by water in air, and that the degree of condensation is around 60% (Table 1).

Fig. 1 gives an example of the effect of contact time t on the ^{29}Si resonance of PMPS(15)–PVI copolymer. Intensities in Fig. 1 reflect local CP dynamics, which may vary from site to site. According to the simple theory in this CP process, magnetization $M(t)$ is expressed as a function of the contact time (t) as follow [17]:

$$M(t) = M_e\left[\exp[-t/T_{1\rho}^{H}] - \exp(-t/T_{SiH})\right] \quad (1)$$

Here, M_e, is the ^{29}Si equilibrium magnetization obtained when both spin systems fully interact with each other without any energy exchange with the lattice, T_{SiH} is the time constant for the energy exchange between ^{1}H and ^{29}Si spin systems, and $T_{1\rho}^{H}$ is the spin–lattice relaxation time in rotating frame. This equation indicates that the ^{29}Si magnetization appears at the rate of the order of $(T_{SiH})^{-1}$ and disappears at the rate of $(T_{1\rho}^{H})^{-1}$.

Fig. 2 shows a semi-logarithmic plot of the peak intensity as a function of the contact time for the silicon in PMPS(15)–PVI copolymer. The values of T_{SiH} estimated by the curve-fittings are summarized in Table 1. It is found that the T_{SiH} values of the T^i species in copolymers

Table 1
The degree of condensation and the T_{SiH} values of the respective resonance lines of the PMPS–PVI copolymers

Copolymers	Degree of condensation (%)	T_{SiH} (ms)/Fraction (%)		
		T^1	T^2	T^3
PMPS(5)–PVI	61.32	0.88/32.3	1.09/51.4	4.04/16.3
PMPS(10)–PVI	65.04	1.12/25.6	0.89/53.7	0.89/20.7
PMPS(15)–PVI	55.90	0.89/42.7	0.84/46.9	0.74/10.4
PMPS(20)–PVI	60.15	0.93/32.1	1.04/55.3	1.62/12.6
PMPS(25)–PVI	58.71	0.89/36.2	0.84/51.5	0.74/12.3
PMPS(30)–PVI	60.45	0.75/32.0	0.73/54.7	0.68/13.3

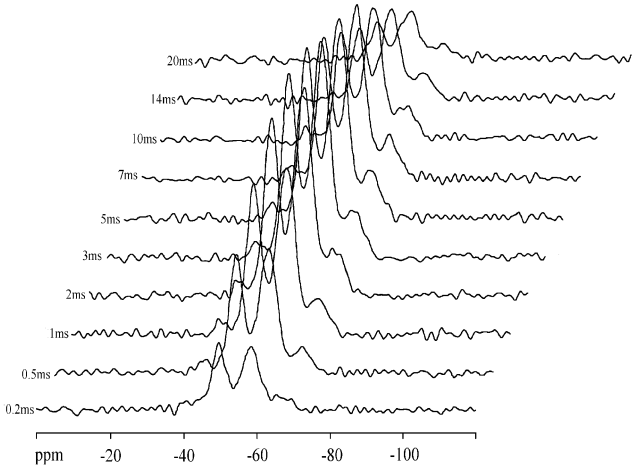

Fig. 1. Stacked plot of the ^{29}Si CP-MAS spectra of PMPS(15)–PVI copolymer as a function of contact time.

are nearly identical. The similar CP efficiency implies that the Si–H dipolar interactions in copolymers is independent of the MPS content. On the other hand, the curve in Fig. 2 is linear suggesting that the ^{29}Si atoms of the T^i species must be within approximately 10 Å of a proton to facilitate polarization transfer [17].

3.2. ^{1}H spin–lattice relaxation time in the rotating frame $T_{1\rho}^{H}$

^{13}C CP/MAS NMR spectra of PMPS–PVI copolymers are nearly identical. The resonance's (Fig. 3) at around 137, 130 and 116 ppm can be assigned to the imidiazole ring, while those at 176, 70, 24, 18 and 10 ppm are due to MPS units. Additionally, the resonance's around 51 and

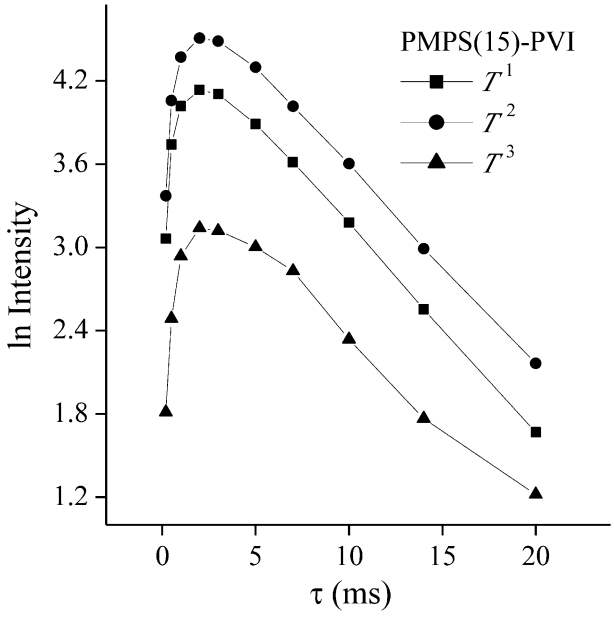

Fig. 2. Semi-logarithmic plot of the peak intensities of the T^i species shown in Fig. 1 as a function of the contact time.

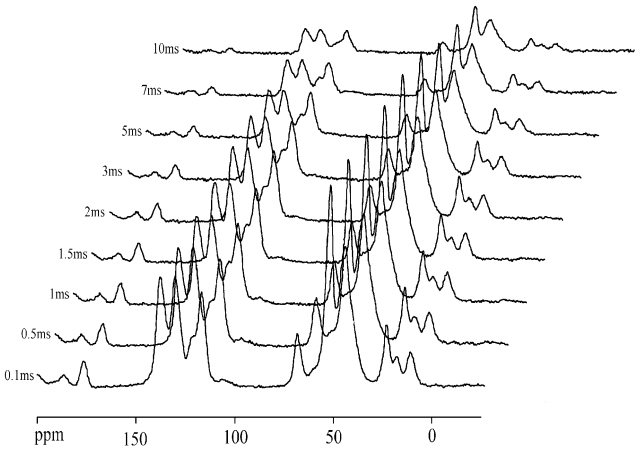

Fig. 3. Stacked plot of the ^{13}C CP-MAS spectra of PMPS(15)–PVI copolymer as a function of delay time.

43 ppm result from overlapping lines from both components. Based on the spin-locking mode employed in ^{1}H spin–lattice relaxation time in the rotating frame $T_{1\rho}^{H}$ measurement, the magnetization of resonance is expected to decay according to the exponential function [17]:

$$M_\tau = M_0 \exp[-\tau/T_{1\rho}^{H}] \quad (2)$$

Here, τ is the delay time used in the experiment and M_τ corresponds to resonance intensity. Fig. 3 shows the effect of delay time τ on the ^{13}C resonance of PMPS(15)–PVI copolymer. The $T_{1\rho}^{H}$ values of the respective carbon of PMPS(15)–PVI copolymer are evaluated from the slopes of Fig. 4 by Eq. (2), and listed in Table 2. It is clear that the average $T_{1\rho}^{H}$ values of the imidazole ring are smaller than those of the MPS units (resonance 176 ppm). The efficient relaxation may be due to the strong π-interaction between the imidazole rings.

On the other hand, the average $T_{1\rho}^{H}$ values of the imidazole ring smoothly decrease with increasing MPS content in copolymers, while $T_{1\rho}^{H}$ values of the MPS units drastically decrease. The observations reveal that the molecular motion of the imidazole ring is less restricted than the MPS units by the crosslinked structure.

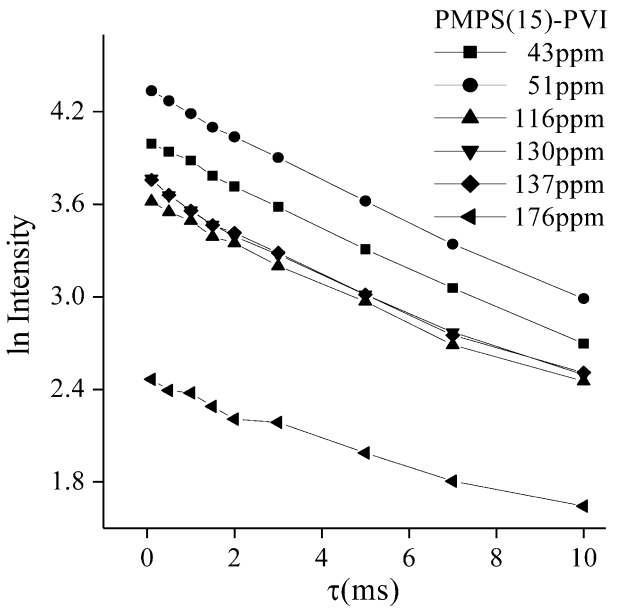

Fig. 4. Semi-logarithmic plot of the peak intensity of PMPS(15)–PVI shown in Fig. 3 as a function of the delay time.

3.3. Thermal analysis

The first scan of PMPS(5)–PVI copolymer shows an exothermal peak at interval of 20–140°C. Maximum peak at 90°C in the exothermal peak is due to water vaporization [11]. However, the second scan shows a glass transition temperature (T_g) at 172°C in PMPS(5)–PVI copolymer suggesting that crosslinking reaction by vaporized water occurred during heating [22]. It is interesting to note that the T_g values of the copolymers decreases with increasing the MPS content (Table 3), although the degree of condensation in PMPS–PVI copolymers is around 60% (Table 1). The result suggests that two types water molecules binding with imidazole units through hydrogen bonding have quite different influence on T_g variation. Type I bound water forms more than one hydrogen bond with imidazole units in copolymer, and Type II bound water forms a single hydrogen bond. Therefore, a lower T_g suggests that Type I bound water decreases with increasing the MPS content in copolymer.

Table 2
$T_{1\rho}^{H}$ values of the respective resonance lines of PMPS–PVI

Copolymers	$T_{1\rho}^{H}$ (ms)						
	43 ppm	51 ppm	116 ppm	130 ppm	137 ppm	Average	176 ppm
PMPS(5)–PVI	8.26	7.41	8.80	7.93	7.67	8.01	29.63
PMPS(10)–PVI	7.37	6.76	7.65	7.26	7.01	7.21	18.00
PMPS(15)–PVI	7.57	7.33	8.30	7.93	7.94	7.81	11.98
PMPS(20)–PVI	5.71	5.88	5.95	5.63	5.80	5.79	7.84
PMPS(25)–PVI	5.61	6.01	6.58	5.32	6.54	6.01	8.25
PMPS(30)–PVI	5.26	5.86	4.61	4.12	4.72	4.91	6.92

Table 3
The thermal characteristic parameters of the copolymer under nitrogen at a heating rate 10°C/min[a]

Copolymers	T_g (°C)	T_m (°C)	Y_c (°C)	n	r_1/r_2		
					van Krevelen	Coats–Redfern	MacCallum–Tanner
PMPS(5)–PVI	172	441	11.96	1.11	0.9949/0.9970	0.9950/0.9937	0.9958/0.9967
PMPS(10)–PVI	169	429	16.12	1.23	0.9980/0.9969	0.9982/0.9944	0.9985/0.9966
PMPS(15)–PVI	163	420	19.35	1.27	0.9979/0.9980	0.9981/0.9968	0.9985/0.9978
PMPS(20)–PVI	–	403	29.31	2.06	0.9984/0.9977	0.9975/0.9948	0.9983/0.9975
PMPS(25)–PVI	159	399	30.45	1.88	0.9974/0.9977	0.9975/0.9937	0.9980/0.9974
PMPS(30)–PVI	–	399	35.08	2.45	0.9963/0.9989	0.9961/0.9963	0.9971/0.9987

[a] T_g: temperature of glass transition, T_m: temperature at maximum rate of weight loss, Y_c: char yield, n: use Kissinger n, r: correlation coefficient.

The TGA curves of PMPS(5)–PVI and PMPS(30)–PVI copolymers under nitrogen are shown in Fig. 5. It clearly shows four main reaction stages in its differential weight loss (DTG) curve. The weight loss of the least stable step is the removal of the water, and its maximum rate temperature is around 150°C. Generally, a polymer with a long side chain has a low ceiling temperature and easily tends to depolymerize because of radical depolymerization. The weight loss at the interval of 200–300°C (second step) is thus attributed to the ester bond decomposed. The third step (300–450°C) and fourth step (>450°C) may be due to the scissions of PVI chain [11] and the hydroxyl condensation [23], respectively. Temperature at maximum rate of weight loss (T_m) decreases with increasing the MPS content, whereas char yield (Y_c) at 700°C increases (Table 3).

3.4. Kinetic analysis

The reaction order n for dehydration and decomposition of the ester bond in copolymers is determined by the Kissingers' equation [23]. The value of n for dehydration is larger than 1.0, and that increases with increasing the MPS content (Table 3). However, the n values of the decomposition of the ester bond are around 1.26.

The degree of conversion α is defined as the ratio of actual weight loss to total weight loss. Evaluating the apparent activation energy of the dehydration (E_{a1}) and the decomposition of the ester bond (E_{a2}) for the copolymers.

Table 3 lists the values of correlation coefficients (r). It is found that the r-values are similar nearly. Therefore, the evaluations using three methods give equally good E_a values. Fig. 6 indicates the values of E_{a1}, corresponding to dehydration water, decrease with increasing the MPS content. The result reveals that Type II bound water, forming one hydrogen bond, increases with increasing MPS content in copolymer, as we have observed in DSC. This water molecule possesses a lower activation energy and is correspondingly easier to remove. On the other hand, the

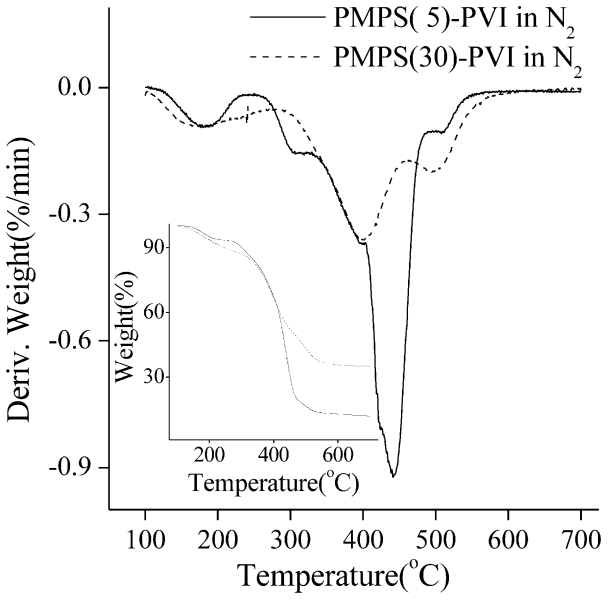

Fig. 5. TGA and DTG thermograms of PMPS(5)–PVI and PMPS(30)–PVI copolymers under nitrogen at a heating rate 10°C/min.

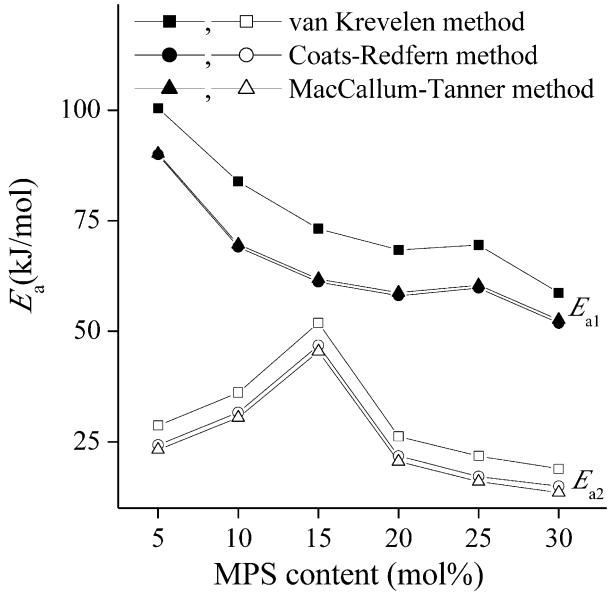

Fig. 6. The dependence of dehydration energy E_{a1} (■, ●, ▲) and ester bond decomposition energy E_{a2} (□, ○, △;) calculated by the van Krevelen (■, □), Coats–Redfern (●, ○), and MacCallum–Tanner (▲, △) method on the MPS content for PMPS–PVI copolymers.

values of E_{a2}, corresponding to the decomposition of the ester bond, estimated by the method of van Krevelen, Coats–Redfern, and MacCallum–Tanner, are approximately 30 kJ/mol.

4. Conclusions

^{29}Si NMR showed that the methoxyl groups in PMPS–PVI were condensation by water in air, and the degree of condensation (~60%) was independent of the MPS content. Moreover, the relaxation times of the energy exchange between ^{1}H and ^{29}Si spin systems (T_{SiH}) of the T^{i} species in copolymers had similar CP efficiency. However, the spin–lattice relaxation time in rotating frame revealed that the chain mobility of the imidazole ring was less restricted than MPS units by the crosslinked structure. The values of T_g and the apparent activation energy for dehydration of water (E_{a1}) of the copolymers were also decreased with increasing MPS content, suggested that the bound water forming a single hydrogen bond with the copolymer increased with increasing MPS content in copolymer. However, the values of E_{a2} of the copolymers, corresponding to the decomposition of the ester bond, estimated by the method of van Krevelen, Coats–Redfern, and MacCallum–Tanner, were approximately 30 kJ/mol and were independent of the MPS content.

Acknowledgements

The authors thank the National Science Council of the Republic of China. We would also like to thank Miss S.Y. Fang and Mr Y.C. Lin for their expert technical assistance.

References

[1] da Costa SLFA, Agostinho SML, Nobe K. J Electrochem Soc 1993;140:3483.
[2] Lewis G. Corros Sci 1982;22:579.
[3] Zucchi F, Trabanelli G, Fonsati M. Corros Sci 1996;38:2019.
[4] Walker R. Corrosion 1973;29:291.
[5] Walker R. Corrosion 1975;31:97.
[6] Lewis G. Corros Sci 1982;22:579.
[7] Zucchi F, Trabanelli G, Fonsati M. Corros Sci 1996;38:2019.
[8] Ishida H, Kelley K. J Adhes 1991;36:177.
[9] Jang J, Ishida H. Corros Sci 1992;33:1053.
[10] Hansen J, Kumagai M, Ishida H. Polymer 1994;35:4780.
[11] Jang J, Kim H. J Appl Polym Sci 1995;56:1495.
[12] Kim H, Jang J. J Appl Polym Sci 1997;64:2585.
[13] Jang J, Jang I, Kim H. J Appl Polym Sci 1998;68:1343.
[14] Jang J, Jang I, Kim H. J Adhes Sci Technol 1998;12:323.
[15] Ruhnau FC, Veeman WS. Macromolecules 1996;29:2916.
[16] Komoroski RA, editor. High resolution NMR spectroscopy of synthetic polymers in bulk. Florida: VCH, 1986.
[17] Mehring M. Principles of high resolution NMR in solids. 2nd ed. Berlin: Springer, 1983.
[18] Chang TC, Wang YT, Hong YS, Chiu YS. J Polym Sci, Part A: Polym Chem 2000;37:1972.
[19] van Krevelen DW, van Herden C, Huntjens F. J Fuel 1951;30:253.
[20] Coats AW, Redfern JP. Nature 1964;201:68.
[21] MacCallum JR, Tanner J. Eur Polym J 1970;6:1033.
[22] Chang TC, Wang YT, Hong YS, Chiu YS. Polym Degrad Stab 2000;69:317.
[23] Kissinger HHE. Anal Chem 1957;29:1702.